J. Fluid Mech. (1967), *vol.* 30, *part* 4, *pp.* 699–722
Printed in Great Britain

The reflexion of a shock wave at a rigid wall in the presence of a boundary layer

By L. F. HENDERSON
Department of Mechanical Engineering, University of Sydney†

(Received 4 May 1967)

The paper discusses the reflexion of a shock wave off a rigid wall in the presence of a boundary layer. The basic idea is to treat the problem not as a reflexion but as a refraction process. The structure of the wave system is deduced by a simple mapping procedure. It is found that a Mach stem is always present and that the bottom of this wave is bifurcated—called a lambda foot. The reflexion is said to be regular if the Mach stem and the lambda foot are confined to the boundary layer and irregular if either extends into the main stream. Two types of regular reflexion are found, one that has reflected compression waves and the other that has both reflected compression and expansion waves. Initial conditions are given that enable one to decide which type will appear. There are also two types of irregular reflexion, one that has a Mach stem present in the main stream and the other that is characterized by a four-wave confluence. Finally there are also two processes by which regular reflexions become irregular. One is due to the formation of a downstream shock wave that subsequently sweeps upstream to establish the irregular system and the other is due to boundary-layer separation which forces the lambda foot into the main stream.

1. Introduction

The interaction of a plane shock wave with a boundary layer in steady flow has been the subject of many experimental investigations. Some of the better-known studies are due to Ackeret, Feldmann & Rott (1946), Liepmann (1946), Fage & Sargent (1947), Bardsley & Mair (1951), Barry, Shapiro & Neumann (1951), Liepmann, Roshko & Dhawan (1952), Gadd, Holder & Regan (1954), Bogdonoff & Kepler (1955), Holder & Gadd (1955), Chapman, Kuehn & Larson (1958), Hakkinen, Greber & Trilling (1959). While this work has undoubtedly led to progress towards understanding the phenomenon, the flow is so complicated that a completely satisfactory theory has not yet been formulated. Various theories of the laminar interaction have received critical discussion by Curle (1962) and by Lees & Reeves (1964). The theory of the turbulent interaction has not been developed to the same extent. The paper by Lees & Reeves gives perhaps the most successful theory currently available. The flow model used in their analysis is shown in figure 1 and it contains the most

† Now on leave at Graduate School of Aerospace Engineering, Cornell University, Ithaca, N.Y.

prominent features of the interaction that have been observed by experiment. However, the details of the wave system in the supersonic part of the boundary layer have been neglected and probably this is the most important gap in present-day knowledge of the phenomenon. Some experimenters have attempted to

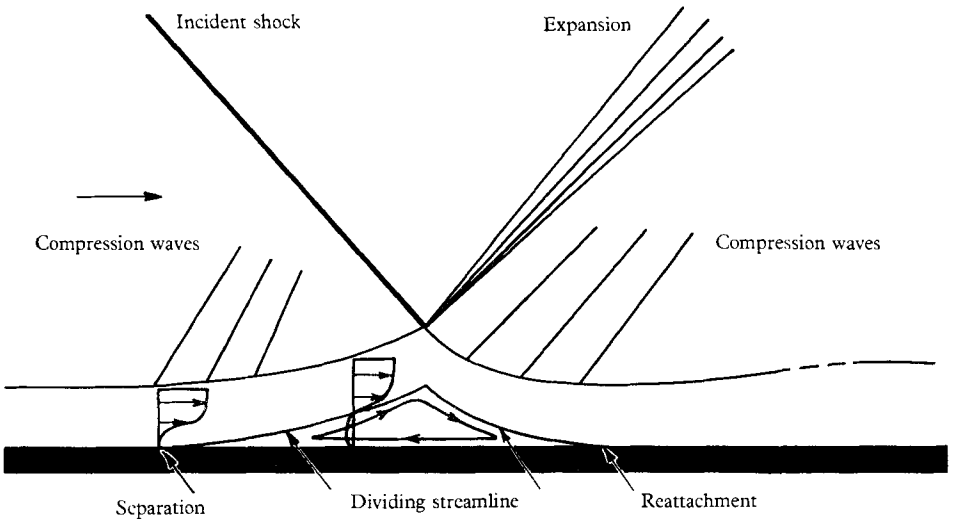

FIGURE 1. Flow model (after Lees & Reeves 1964).

sketch the wave pattern in this area, the most comprehensive attempt being due to Bogdonoff & Kepler (1955). The objective of the present paper is to construct a reasonably complete picture of the entire structure of the interaction including in particular the wave pattern inside the boundary layer. The basis of the analysis is to treat the phenomenon as the *refraction* of a shock by a boundary layer which is represented by an inviscid shear layer. The methods that will be used here have been previously applied by the present writer (Henderson 1966) to the refraction of a shock wave at an interface, or boundary between two different gases.

2. Shock-wave refraction

A systematic series of experiments on shock-wave refraction has been carried out by Jahn (1956). The theory of the phenomenon has been discussed by the present writer Henderson (1966). Following this work it is convenient to classify the wave systems into three groups (figure 2). In the first group the incident shock i is refracted at the interface and this results in a transmitted wave t which is always a shock and a reflected wave which may be either a shock r or a Prandtl–Meyer expansion e. These two wave systems comprise the regular group and they are characterized by a well-defined refraction point Q and by the property that all waves lie along straight rays that emanate from that point. The flow in the vicinity of Q can be determined by constructing the shock polars and characteristic curves for the wave system in the hodograph $(P/P_0, \delta)$-plane. It can be shown by the analysis that there is in general a different entropy

path on the one hand for the flow crossing the transmitted shock and on the other for the flow crossing the incident and reflected waves. One physical consequence is that a vortex sheet, or slip line, begins at Q.

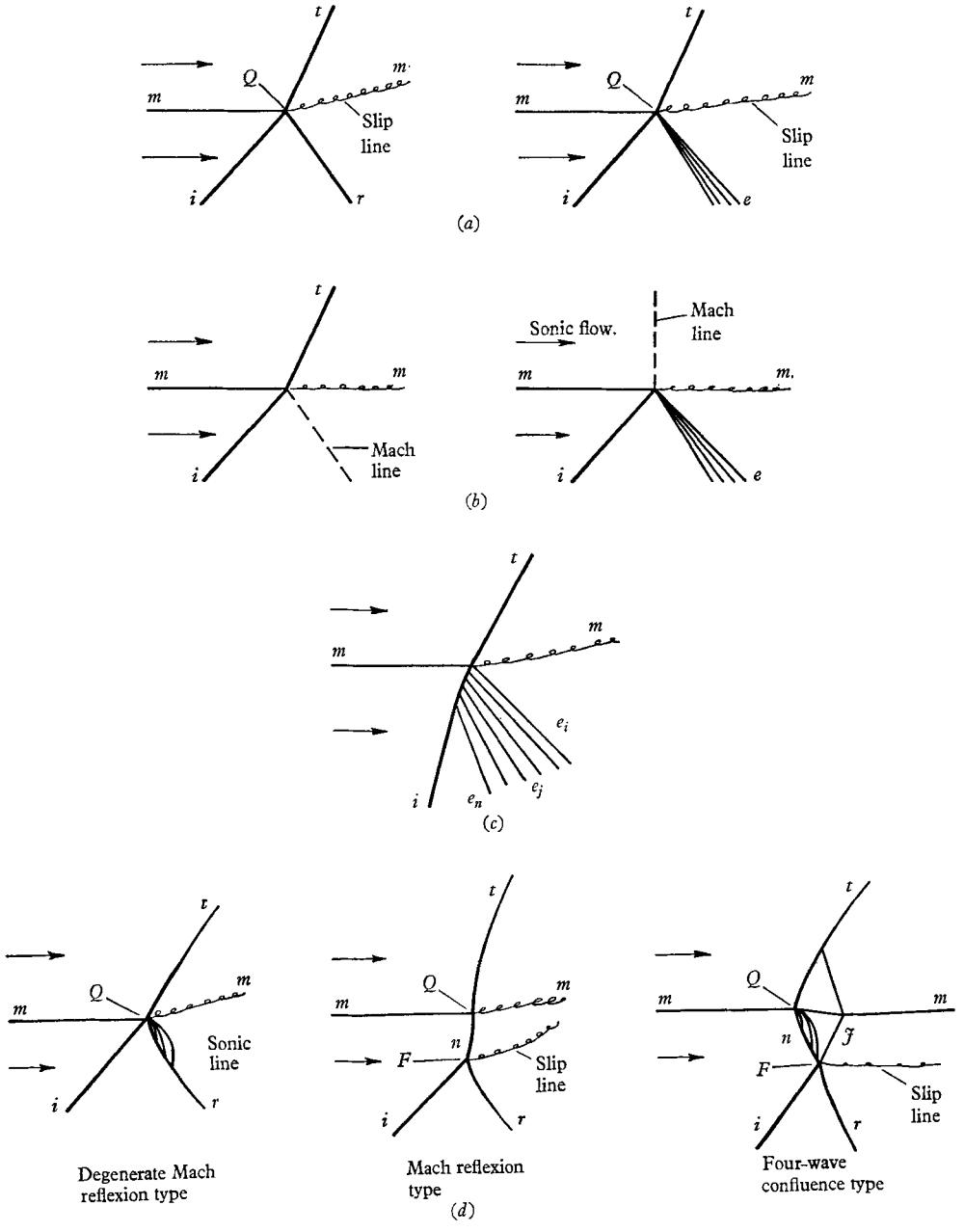

FIGURE 2. Wave refraction systems at a gas interface. *mm*, interface; Q, refraction point; F, confluence point; *i*, incident shock; *t*, transmitted shock; *r*, reflected shock; *e*, reflected expansion. (*a*) Regular group. (*b*) Degenerate group. (*c*) Fast–slow irregular refraction. (*d*) Slow–fast irregular refractions.

If the reflected wave is a shock the flow near Q can be described by a single polynomial equation of degree 12 (Henderson 1966). The state of the gas can be found from a particular real root of the polynomial. For a refraction at a Mach number interface the initial conditions sufficient to define the coefficients of a polynomial, and therefore a set of roots, may be taken to be (γ, M_{00}, M_{01}, P_1/P_0). It often happens that for given initial conditions several wave systems having either reflected shocks and/or reflected expansions are available as feasible physical alternatives. If all the possibilities are arranged as an ordered set in ascending order of magnitude and compared with experiment then it is found that it is the weakest member of the set that actually appears (Henderson 1966). The strength or magnitude of a solution is measured by the pressure ratio across the transmitted shock.

If the initial conditions are gradually and continuously altered then it sometimes happens that one of the waves in a regular system will degenerate to a Mach line. The second group of refractions consists of the various types of regular systems that contain a degenerate wave. The third group are merely those that do not fall into the above categories and they are collectively called the irregular group. A further classification can be made by reference to the relative speeds of sound in the two media. For example if i is in a medium where the speed of sound is a_i and t is a medium where it is a_t, then the refraction is called 'slow-fast' if $a_i < a_t$ and 'fast–slow' if $a_i > a_t$. The regular and degenerate wave systems are essentially the same for both the slow–fast and fast–slow combinations of media but there are differences in the irregular group. These are shown in figures 2*c* and 2*d*, which include all the known types.† Degenerate wave systems are often but not always encountered during transition from a regular to an irregular system or vice versa. Furthermore, a degenerate system is often but not always found to be associated with a multiple root of the polynomial. So far as it is known an irregular system only appears for those initial conditions for which regular systems are impossible. This may be brought about for example by real roots of the polynomial becoming unreal or by the real roots requiring that one of the waves in the system becomes a thermodynamically impossible expansion shock. A more detailed discussion of these matters is given in our earlier paper.

3. Refraction of a shock wave by a boundary layer

3.1. *Structure of the regular part of the refraction*

Inside the boundary layer the Mach number decreases continuously and monotonically from the value it has at the free stream to zero at the wall. Between these limits a sonic line exists that effectively divides the boundary layer into a subsonic and a supersonic part. For analytical purposes the continuous Mach number distribution is approximated by an incremented profile so that the boundary layer is supposed to consist of thin parallel streams of inviscid gas with a small change in the Mach number between one stream and the next. Specifically the effects of viscous mixing between the streams is neglected. If an incident

† Further work has extended and corrected the theory of the irregular wave systems, particularly of the fast–slow irregular group, Henderson (1967).

shock i strikes the outer edge of this idealized boundary layer as in figure 3 then it will be refracted by the first incremental change in the Mach number. Consequently there will appear a transmitted shock t_1 and either a reflected shock r_1 or a reflected expansion e_1. At the next Mach number increment the wave t_1 will itself be refracted, causing the shock t_2 to appear together with a reflected wave r_2 or e_2. In this way it may be seen that as i is refracted it penetrates the boundary layer and becomes a curved shock t_j which emits a band of reflected waves r_j or e_j. Further information on the nature of the wave system can now be obtained from the hodograph diagram.

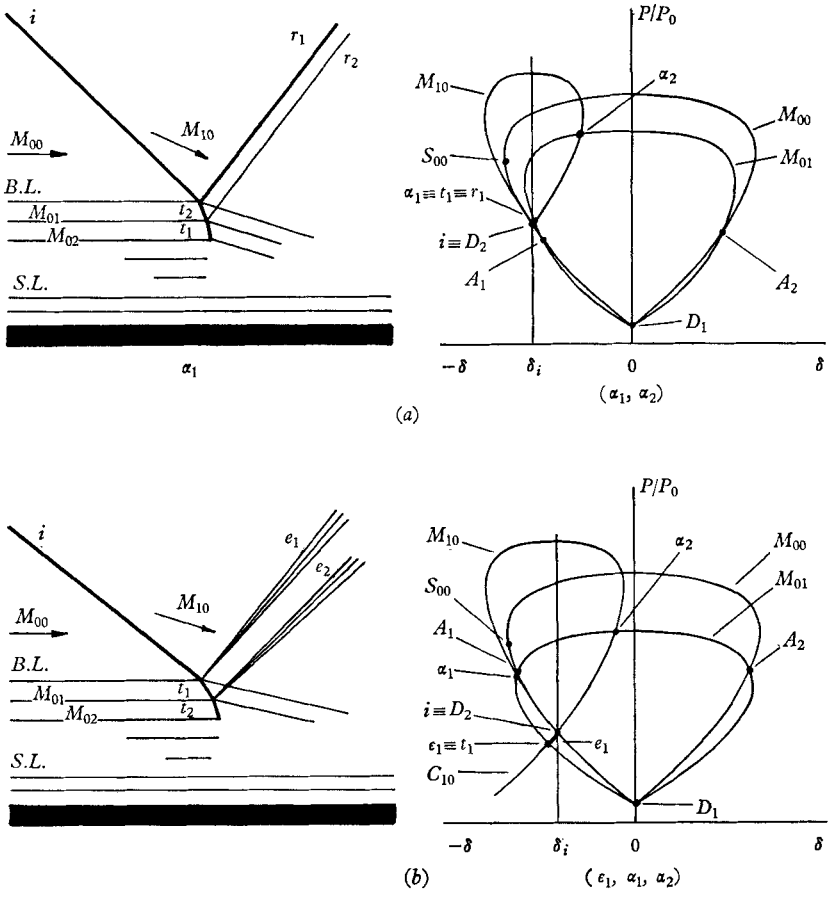

FIGURE 3. Conditions for a reflected shock or a reflected expansion. (*a*) Reflected shock. (*b*) Reflected expansion.

Construction of the diagram is commenced by plotting the shock polars for the Mach numbers M_{00} and M_{01}. In general the polars will be found to intersect at the symmetric points A_1, A_2 and at the double point D_1. This latter point represents the initial state of both streams. The wave i maps into a point D_2 on polar M_{00} and the position of D_2 will be determined by the initial conditions. The polar and the characteristic for the Mach number M_{10} are plotted next and both curves start from D_2. The geometry of the diagram is such that if D_2 has a

larger ordinate than A_1 then the only regular solutions (roots) are α_1, α_2 both of which correspond to a regular wave system with a reflected shock. The ordered set is therefore (α_1, α_2). If, however, D_2 lies below A_1 then the characteristic curve leads to an extra solution ϵ_1 which corresponds to a regular system with a reflected expansion. The ordered set is now $(\epsilon_1, \alpha_1, \alpha_2)$. The ordinate of A_1 can be calculated as shown in the appendix and is given by

$$P_1/P_0 = M_0^2 - 1. \tag{1}$$

One observes that this equation is independent of the ratio of specific heats γ. The curve is shown in figure 4.

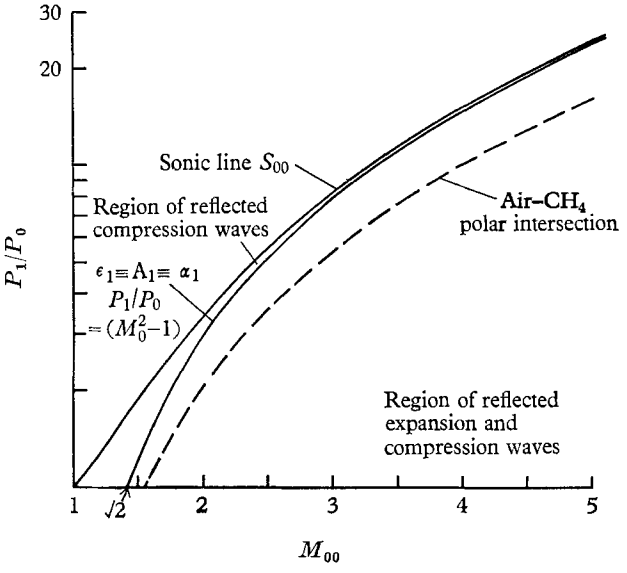

FIGURE 4. Initial conditions for reflected compression and expansion waves.

Consider now the (α_1, α_2) set and in particular the α_1 solution. This solution may be constructed for the refraction of t_j at each Mach number increment. When this is done it is found that α_1 moves along the successive polars for M_{0j} and gradually approaches the sonic point S_{0j} (figure 5*a*). With decreasing M_{0j} the pressure ratio across t_j increases and the shock thus becomes stronger and steeper as it penetrates. While this is happening the polar M_{1j} for the reflected shock is steadily shrinking.† The process terminates when α_1 becomes coincident with S_{0n}, denoted by $\alpha_1 \equiv S_{0n}$. Physically this condition corresponds to sonic speed downstream of t_n and the wave r_n becoming a Mach line degeneracy. At the coincidence the polar M_{1n} shrinks into the point S_{0n}. Further penetration will require subsonic flow downstream of the transmitted shock and a reflected shock will then be impossible. It is concluded that the regular refraction extends only to the sonic point $t_n \equiv S_{0n}$ and that beyond this point the refraction becomes irregular. The reflected waves r_j are propagated towards the main stream and are refracted by the part of the boundary layer that they

† The diagram was too crowded to show the M_{1j} polars clearly and they were therefore omitted.

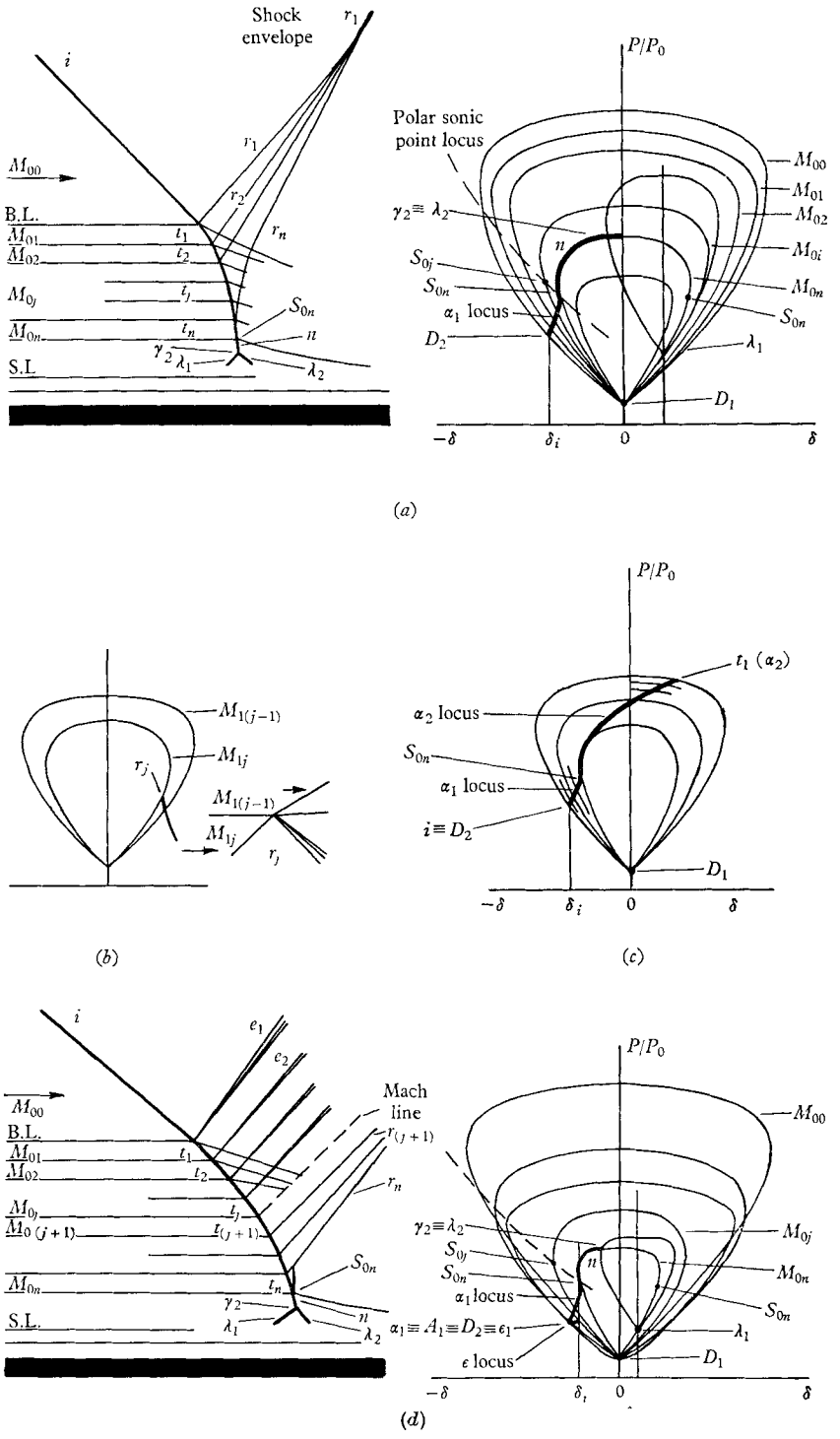

FIGURE 5. Refraction of the incident shock wave i. (*a*) Refraction with reflected compression waves. (*b*) Refraction of r_j. (*c*) Locus of α_1 and α_2. (*d*) Refraction with reflected expansions and compressions.

cross. A typical refraction of r_j gives rise to a transmitted shock and a reflected expansion (figure 5*b*) and the r_j are weakened as they are propagated. The regular part of the refraction thus forms a wave net which can be determined from the hodograph diagram and the polynomial. Ultimately the r_j emerge from the boundary layer and envelope into a shock wave r^1 in the main stream.

The wave i maps into a point D_2 which is continuous with the α_1 locus and in fact it is one of the end-points of the locus. This means that in the physical plane i and t_j (α_1) can be regarded as forming a continuous single shock which begins to emit compression waves of small intensity as it enters the boundary layer. However, the same continuity does not exist between i and t_j (α_2), see figure 5*c*; the maps of these waves are in fact discontinuous with respect to each other. In the physical plane the α_2 solution requires that the vanishingly small Mach number increment at the edge of the boundary layer must discontinuously produce a shock t_1 that is in general much stronger than i and also a reflected shock r_1 of finite strength. It is also implied that the wave angles of i and t_1 (α_2) can be substantially different. It is contrary to accumulated experience that a shock propagating through an indefinitely small Mach number gradient will suddenly exhibit a large change in its pressure ratio and its wave angle. Clearly of the two alternatives (α_1, α_2) the α_1 solution is the only feasible choice.

When the initial conditions place D_2 below A_1 the ordered set becomes (ϵ_1, α_1, α_2). The hodograph diagram reveals that both the α_1 and α_2 solutions are discontinuous with respect to the map of i and that the only solution which is continuous with i is ϵ_1. On the basis of previous argument the ϵ_1 solution is to be selected. A further argument in favour of the ϵ_1 solution can be developed as follows. The boundary-layer refraction is the slow–fast type† and with respect to our previous work on the gas interface (Henderson 1966) it is analogous to the air–CH_4 combination. The curve corresponding to the A_1 curve is shown in figure 4. The region of initial conditions that lie below this curve require the (ϵ_1, α_1, α_2) set for both gas combinations. One can now imagine that the following fictitious experiment is performed on the M_{00}–M_{01} interface of the boundary layer. The M_{01} stream is gradually and continuously diluted with methane until it consists entirely of this gas. There will be corresponding gradual and continuous changes in the hodograph diagram and in particular the polar intersection A_1 will move slowly down the diagram until the A_1 curve is changed into the air–CH_4 curve (figure 4). Now the experimental results for the air–CH_4 refraction agree with the ϵ_1 solution; hence by continuity this solution must also be appropriate to the air–air interface for the analogous region of initial conditions. The position now is that when D_2 lies above A_1 there will be a regular refraction with a reflected shock and when D_2 lies below A_1 there will be a regular refraction with a reflected expansion. In the special case when D_2 and A_1 are in coincidence the reflected wave is a Mach line and the system is degenerate.

The maps of the refraction with a reflected expansion are shown in figures 3*b* and 5*d*. The hodograph diagram shows that, as t_j penetrates, the intersection

† Because $a_j < a_{j+1}$.

point A_{1j} between successive pairs of polars moves towards D_1 until there is the coincidence $\epsilon_1 \equiv A_1 \equiv D_2 \equiv \alpha_1$. The physical consequence is that the waves e_j weaken steadily as t_j penetrates until they finally degenerate to a Mach line at the coincidence. With further penetration D_2 lies above A_1 and the refraction becomes an α_1 type with reflected compression waves. From here on the situation is similar to that shown in figure 5*a*. The map of t_j exhibits a cusp in the hodograph plane at the Mach line degeneracy, the lower branch of the map corresponding to reflected expansions and the upper branch to reflected compressions.

3.2. *Structure of the irregular part of the refraction*

Consider now the irregular wave system at the foot of the shock t_j. The incident wave is t_n and the refraction will occur at the M_{0n}–$M_{0(n+1)}$ interface. By once again appealing to the fictitious experiment† it may be concluded that the irregular refraction is one of the types shown in figure 2*d*. This, however, is on the tacit assumption that the wall does not alter the wave system in any essential manner. The problem therefore is to find out what effect the close proximity of a rigid wall is likely to have upon these systems. To begin with consider an isolated flow with a single Mach number interface in which the initial conditions require the appearance of the four-wave confluence type of irregularity. If in the initial state all boundaries are at infinity then the maps will be as shown in figure 6*a*. Maps similar to these ones have been discussed in detail previously (Henderson 1966). In a real flow it would be expected that the waves t_{n+1} and r would become Mach lines in the far field due to their being overtaken by following expansion waves. The same thing is assumed to happen here although it is not essential to the argument. The point infinity maps into D_1 for t_{n+1} and D_2 for r and the shocks themselves map into the polar segments QBD_1 and FD_2 respectively. The hodograph diagram shows that t_{n+1} is inclined forward of the refraction point Q and strengthens continuously as it propagates until it becomes normal to the flow at B. Beyond B it weakens continuously, ultimately becoming a Mach line at infinity. In Jahn's experiments on this wave system at the air–methane interface the shock segment QB could be detected although it was not very pronounced, see plate 7 of his paper. Now suppose that a rigid wall is brought from infinity to a position close to the refraction point Q as in figure 6*b*. For an inviscid gas the wave t_{n+1} must now be normal to the wall at B and its polar segment is reduced to QB but the remainder of the hodograph diagram is unaltered. The same result may be obtained from Jahn's experiments, for when he placed a wall near the interface the effect was to reduce the transmitted shock to the segment QB but without altering the nature or structure of the shock system, see plate 8 of his paper. Thus the effects that the wall has on the wave system are to terminate t_{n+1} at the normal shock point B and to enlarge the scale of t_{n+1} in the vicinity of Q, but there is no change in the structure of this irregular system.

The next problem is to find out how this system must be modified in order to

† In this case the $M_{0(n+1)}$ stream is gradually and continuously replaced by methane.

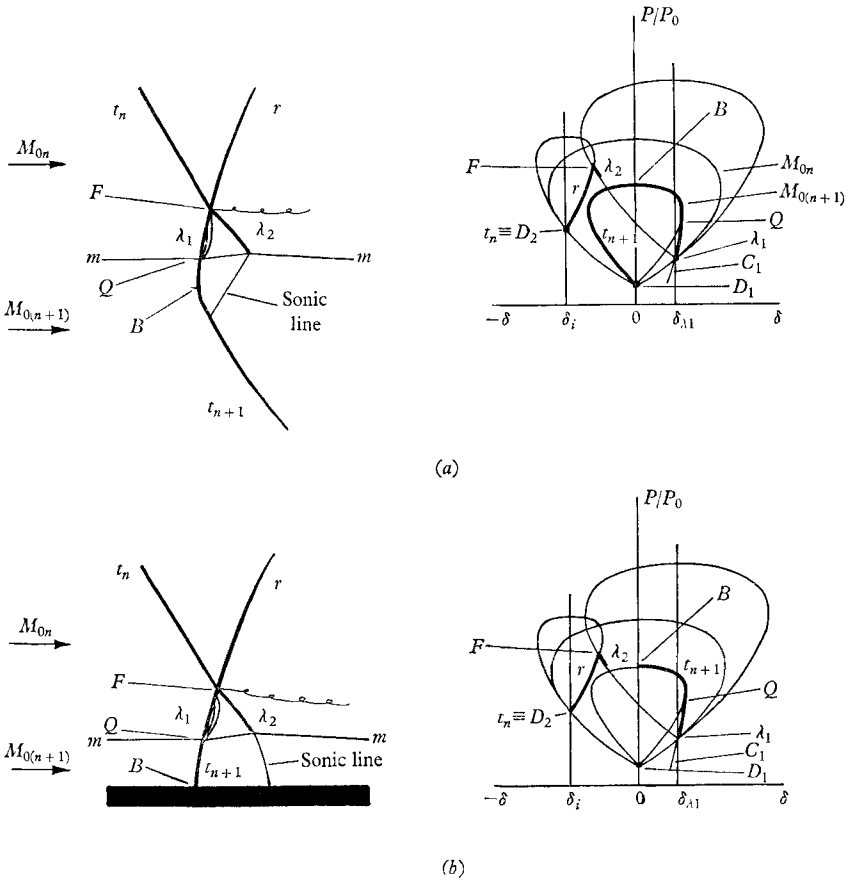

FIGURE 6. Wall effect on four-wave confluence irregular refraction.
(*a*) Walls at infinity. (*b*) Wall near interface *mm*.

fit the conditions at the bottom of the wave t_j that is at t_n. In this connexion it will be recalled that the flow is at sonic speed downstream of t_n. As a preliminary, consider the four-wave confluence illustrated in figure 7. The first pair of maps show the regular intersection of two incident shocks i_1, i_2 and there are two solutions (β_1, β_2) available to describe conditions near the wave confluence point. The weaker β_1 solution is considered to be physically appropriate. When all boundaries are at infinity the reflected waves r_1, r_2 will map into the polar segments $\beta_1 D_2$ and $\beta_1 D_3$ respectively. Now suppose that i_1 is gradually and continuously strengthened while i_2 remains unchanged. This will cause D_2 to move around the polar towards the sonic point S_1 and at the same time the polar for the reflected wave r_1 will begin to shrink. As the process continues β_1, β_2 come into coincidence $\beta_1 \equiv \beta_2$ and with further development they become unreal. When this happens a gap opens in the diagram in the sense discussed by Guderley (1947, 1962), Kawamura & Saito (1956) and Henderson (1966). The physical result is a double Mach reflexion system that contains two confluence points γ_1, γ_2 each of three waves. The Mach stem

n maps into the polar segment $\gamma_1\gamma_2$. With continued development D_2 eventually forms the coincidence $D_2 \equiv S_1$ and the polar for r_1 shrinks into this point. There is now sonic speed downstream of i_1 and r_1 is degenerate. The irregular and degenerate wave system that has now been obtained has the appearance of a

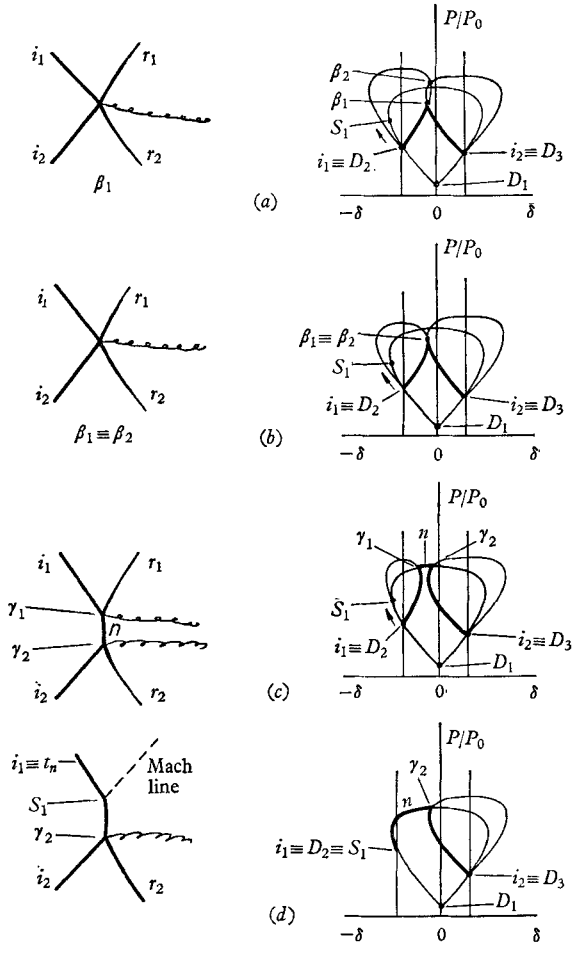

FIGURE 7. Development of an irregular and degenerate four-wave confluence.

single Mach reflexion system. In fact all that one has to do in order to convert it to a conventional Mach reflexion is to strengthen i_1 still further so that the point D_2 moves on to the subsonic part of the free-stream polar. It can now be seen that the degenerate system figure 7*d* actually lies on the transition between the Mach-reflexion and four-wave confluence types and in this sense the system is structurally unique. It is concluded that the only known irregular wave system that can be fitted to t_n is the degenerate system shown in figure 7*d*. It has been added to the boundary-layer maps in figure 5. The wave t_j thus branches into a lambda foot once it propagates beyond t_n.

A hodograph paradox

For the lambda foot to exist the flow downstream of its front wave λ_1 must be supersonic but this makes it impossible for λ_1 to be propagated ahead of the confluence point γ_2. Accordingly, if λ_1 exists it must be propagated *towards* γ_2 and not *away* from it. In these circumstances λ_1 would form as a result of disturbances that originate in the upstream boundary layer and not by disturbances from the incident shock i. The hodograph diagram lends further support for this view because it shows that the initial conditions $(\gamma_1, M_{00}, P_1/P_0)$ which are sufficient to define i and the regular part of the refraction are not sufficient to define the strength or pressure ratio of λ_1. In fact, the strength of λ_1 can be varied within considerable limits $D_1 < \lambda_1 < S_{0n}$ (figure 5), without having any effect on the hodograph map of i or the regular part of the refraction. A similar situation is shown in figure 7, where i_1, i_2 can be varied independently inside wide limits. Within this context one concludes that the shock/boundary-layer interaction is the result of two primary and more or less independent disturbances, one being the incident shock i and the other being the wave λ_1 which is formed from disturbances that arise in the boundary layer. This picture is unsatisfactory because it is physically evident that λ_1 cannot exist and be of finite strength unless i also exists and is of finite strength. Presumably what actually happens is that the initial disturbance from i is transmitted through the supersonic part of the boundary layer into the subsonic part, where it spreads out both upstream and downstream, the upstream disturbances leading to the formation of λ_1. The paradox thus arises because the present methods cannot deal with the history of the flow but only with the final equilibrium state. A knowledge of the behaviour of the subsonic layer is needed here but this is thought to be outside the scope of the present study.

Fine structure of the lambda foot

The next problem is to find out how the upstream disturbances produce λ_1. For this purpose it will be assumed that the supersonic disturbances (waves) originate on the upstream boundary-layer sonic line. Now any wave that begins on a sonic line must not only be vanishingly weak but, as shown by Guderley (1947, 1962), it must also be a compression wave. Hence λ_1 is evidently formed by an envelope of compression waves that begin on the sonic line (figure 8). The present methods are not sufficiently quantitative to determine the distribution of this envelope or in consequence the initial strength of λ_1. This would require a knowledge of the pressure distribution along the sonic line and would have to be obtained from the theory of the subsonic layer. It will be noted, however, that the pressure increases along the sonic line and this will require a corresponding increase in the thickness of the subsonic layer. The discussion will now proceed on the assumption that λ_1 begins at some arbitrary state represented by the point L_1 in figure 8.

As λ_1 propagates towards γ_2 it is refracted because of the monotonic increase in the Mach number from L_1 to γ_2. The hodograph diagram shows the refraction

to be regular and the type that emits expansion waves; λ_1 will therefore weaken as it propagates and its wave angle will become smaller. The expansion waves emitted by λ_1 are propagated towards the wall and in the process are weakly refracted. They also become steeper and eventually make a normal intersection with the sonic line.† At the sonic line they are reflected as compression waves in accordance with the principles established by Guderley. These compression waves are propagated back to λ_1 and begin to strengthen it. As more and more

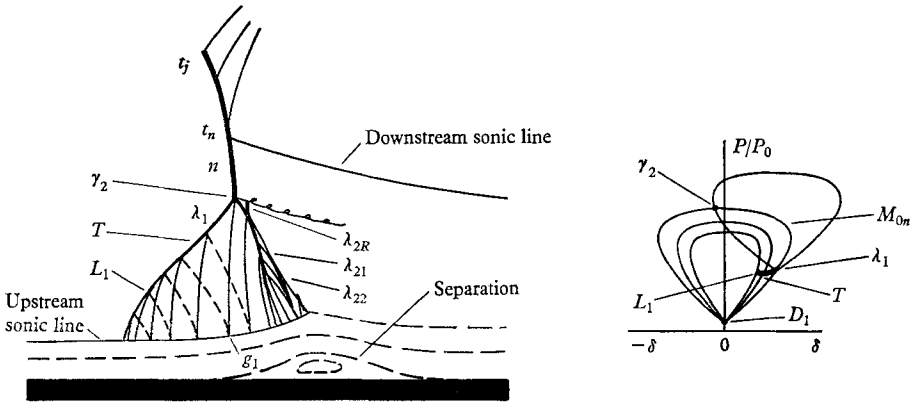

FIGURE 8. Fine structure of the lambda foot.

of them overtake λ_1 the accumulated effect is to induce a point of inflexion T in the wave which is also a minimium point in the hodograph diagram. The final compression wave that intersects λ_1 has been sketched; it is labelled $g_1\gamma_2$. Waves downstream of $g_1\gamma_2$ intersect the back wave λ_2, causing it to steepen.

The wave λ_2 begins at the confluence γ_2 as a result of the interaction of λ_1 and n. It is in general a second family wave which is also refracted as it propagates towards the sonic line. The refraction may be initially regular and if so compression waves will be emitted and these waves will envelope into a weak reflected shock λ_{2R}. Eventually the refraction becomes irregular and λ_2 bifurcates. The position is somewhat analogous to the circumstance at t_n. The front wave of the bifurcation λ_{21} is again formed by compression waves starting on the sonic line. Interaction of λ_{21} with λ_2 will produce the new back wave λ_{22} and this will in its turn bifurcate and so on. All of these waves form in a flow that is already complex and they will be less clearly defined than other waves in the system such as λ_1 or n. The back wave λ_2 is therefore a rather untidy structure consisting approximately of a diffuse double Mach reflexion system which gradually peters out as it approaches the sonic line. The details in the hodograph plane could not be constructed very satisfactorily and are omitted from figure 8. The maps may now be added to the overall picture as shown in figure 9.

† This implies that the sonic line is a streamline. This should be nearly true, because it would be expected that the inclination of the sonic line to the streamline would be very small.

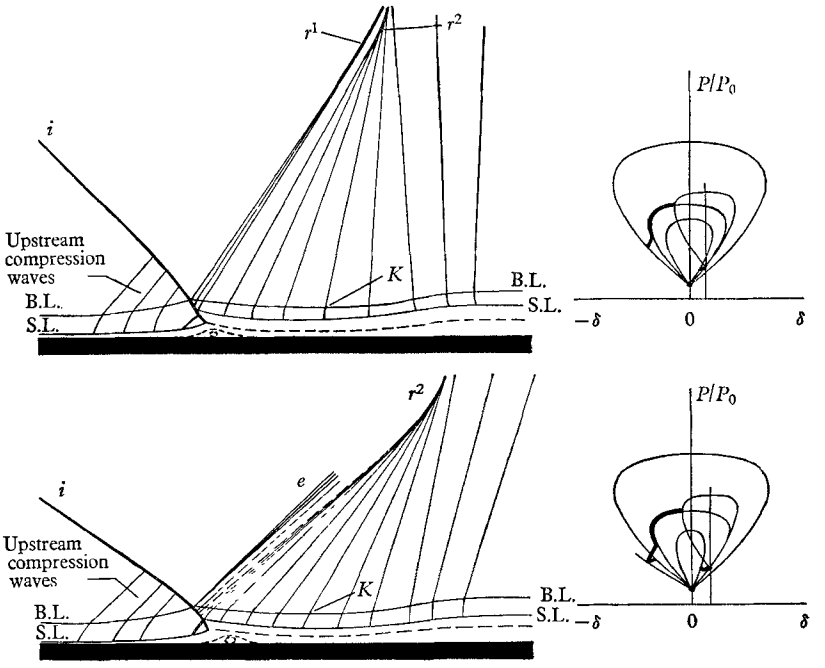

FIGURE 9. Regular refractions with upstream and downstream influence.

4. Downstream influence and Mach reflexion

The theory of the reflexion of a shock wave at a rigid wall in an inviscid gas predicts that the regular reflexion becomes irregular—called Mach reflexion—with the appearance and growth of a Mach stem. The flow is deflected towards the wall by the incident shock and is then brought back parallel to it by the reflected shock. According to the theory, the Mach stem is forced to appear when the reflected shock is unable to match the deflexion caused by the incident shock. Development is similar to that shown in figures 7 *a–c*. Details of the fine structure of the transition are available elsewhere (Guderley 1947, 1962; Kawamura & Saito 1956). The inviscid model is inadequate for a real gas which has a boundary layer along the wall. For example, from the discussion already given it can be asserted that a Mach stem $t_j n$ is always present even when the reflexion is regular. This makes it necessary to revise the definition of regular and Mach reflexion, and the following will serve for the present. The reflexion will be called regular if $t_j n$ is confined to the boundary layer and irregular if it extends into the main stream. The problem now is to find out what circumstances force $t_j n$ to grow.

One begins by noting two important facts about the wave system. First, the main-steam flow is deflected towards the wall by the shock i (figure 9) but sooner or later the flow must be brought back parallel to the wall at some point K by the requirements of continuity. The experimental evidence is that this is accomplished by a system of compression waves which appear downstream of the interaction. This fact is well known and has been mentioned by many

writers, for example Curle (1962) and Lees & Reeves (1964). Evidently these waves begin on the downstream sonic line and envelope to form the main-stream reflected shock r^2. Typical hodographs of the system are shown as the auxiliary maps of figure 11. Secondly, consider two incident shocks i_1, i_2 having the same (γ, M_{00}) but different strengths $P_1/P_0|_2 > P_1/P_0|_1$, see figure 10. Now because both hodographs terminate on the polar sonic point locus the weaker

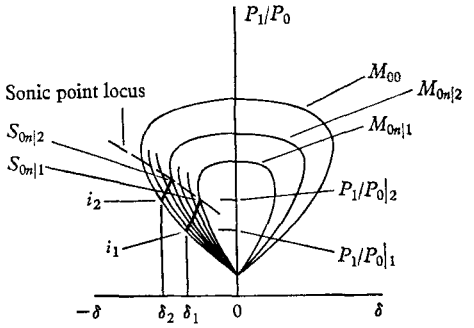

FIGURE 10. Comparison of hodographs of shocks of different strengths $P_1/P_0|_2 > P_1/P_0|_1$ but same (γ, M_{00}).

wave must end on a polar of smaller Mach number than the stronger wave. This leads to the interesting conclusion that the weaker wave will penetrate the boundary layer more deeply before becoming irregular than the stronger wave. As a particular example a Mach line will not become irregular at all and will penetrate all the way to the sonic line as shown in figure 11*a*.

Consider now the sequence of events that will be obtained when i is initially a Mach line and is then gradually and continuously strengthened until it becomes a normal shock. During this development the other initial conditions (γ, M_{00}) will be held constant. For simplicity it will be assumed that the regular part of the refraction generates only compression waves. The initial state is shown in figure 11*a*. Since a Mach line must make the Mach angle to the flow everywhere, it becomes steeper as it penetrates and ultimately becomes normal to the flow at the sonic line. At the sonic line it is reflected reversibly† because of its isentropic character. When i is strengthened into a shock (figure 11*b*) then the wave system which develops is the regular reflexion type that has already been discussed. The wave i deflects the main-stream flow through the angle $-\delta_i$ and the downstream compression waves then bring it back parallel to the wall at some point K. The flow is deflected through the angle ν by these waves so that, at K, $-\delta_i + \nu = 0$. As i is gradually strengthened the penetration of t_j becomes smaller and the lambda foot grows steadily. At the same time $|-\delta_i|$ increases, requiring an equal and opposite response from the compression waves. The latter system therefore strengthens and the Mach number downstream of it M_{-00} becomes smaller. Eventually the stage is reached where ν is equal to the Prandtl–Meyer angle for the Mach number M_{10}, $\nu = \nu_{\max}$

† The reflexion is symmetrical.

as in figure 11*c* for this condition $M_{-00} = 1$. With further development the compression waves are no longer able to match the deflexion across i and the shock envelope r^2 strengthens and moves towards the boundary layer and then

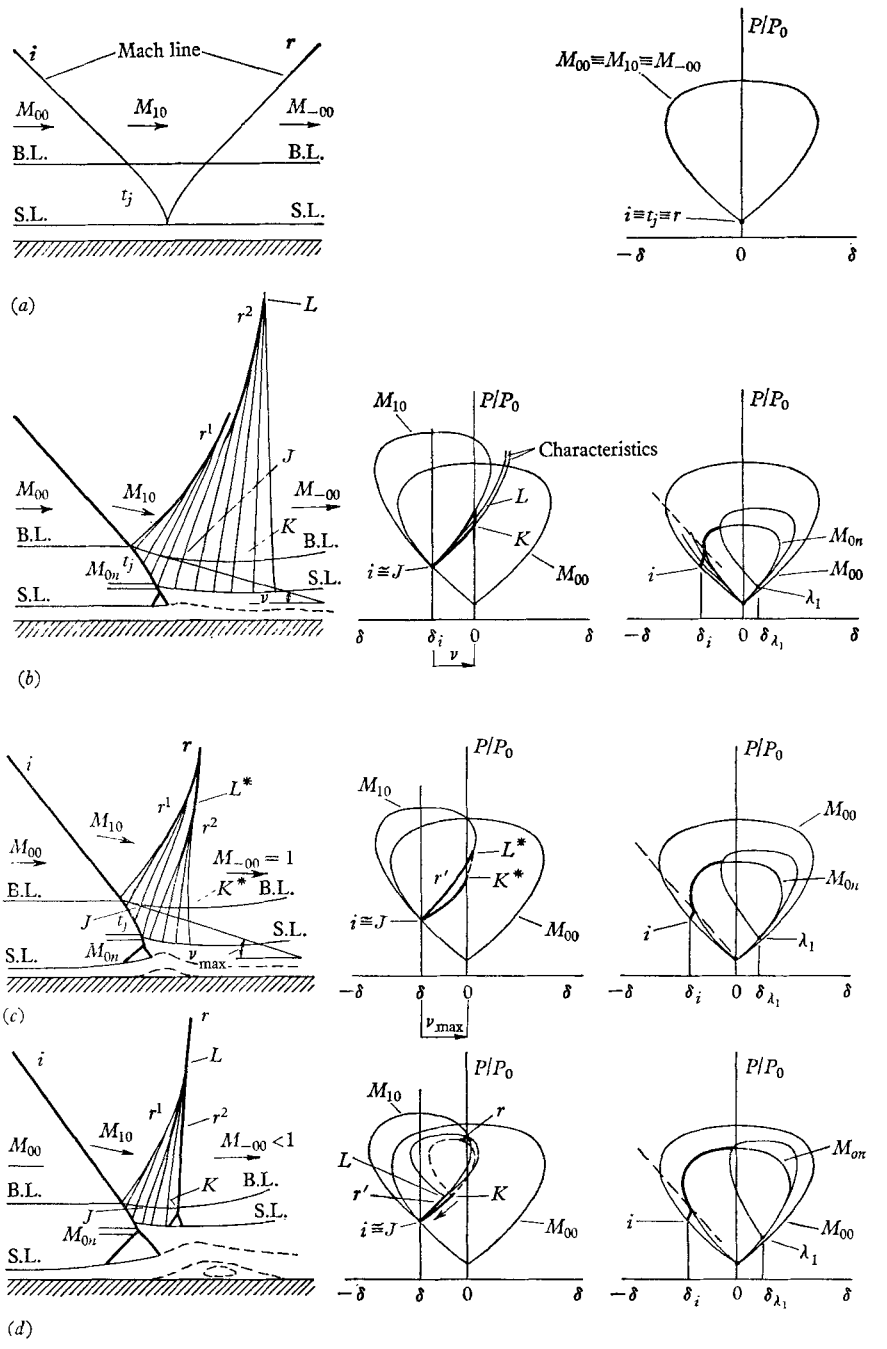

FIGURE 11 (*a–d*). Development of irregular reflexion—Mach reflexion type.

enters it (figure 11 *c*, *d*). An auxiliary hodograph plane has been constructed for these events. The wave r^2 is itself refracted by the boundary layer and will have a lambda foot.

As the strenth of i continues to increase there must be a corresponding increase in the strength of r^2 and this comes about by its moving upstream and overtaking compression waves. The development also involves interactions

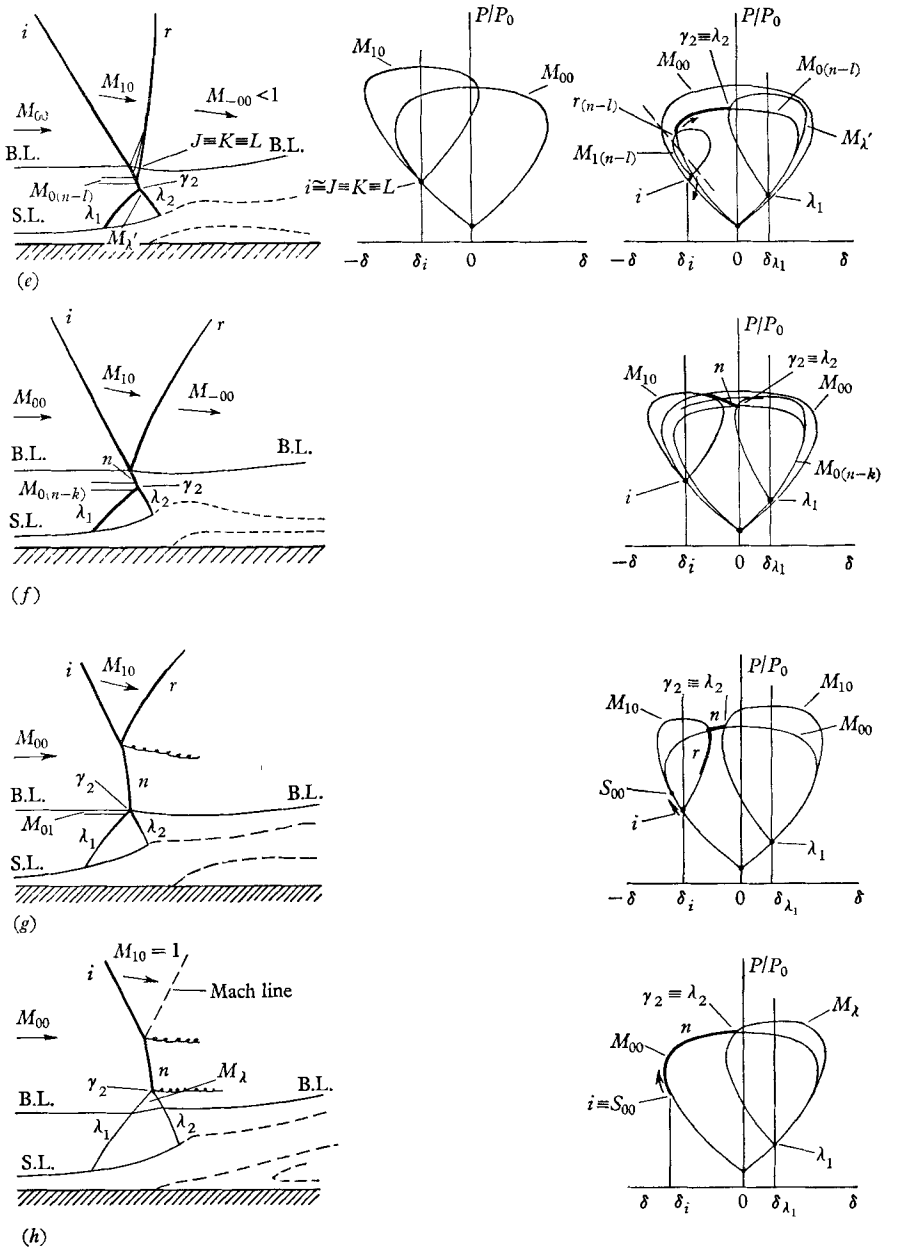

FIGURE 11 (*e–h*). Development of irregular reflexion—Mach reflexion type.

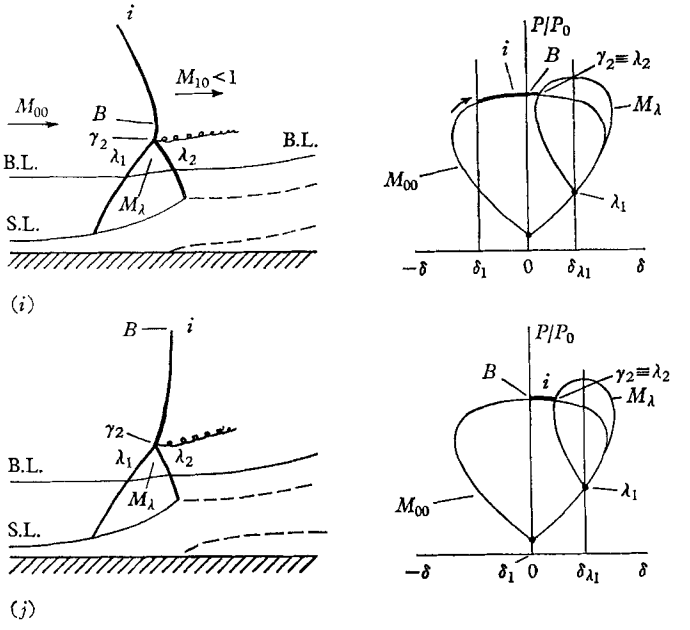

FIGURE 11 (*i–j*). Development of irregular reflexion—Mach reflexion type.

with r^1. The upstream movement† of r finally sweeps up all the compression waves (figure 11*e*) and there is now subsonic flow everywhere downstream of the wave system. As the strength of i is increased still further r begins to climb up t_j; the process is shown partly developed in figure 11*e*. The arrival of r at the foot of t_j causes the compression waves to strengthen into a shock at t_n and a three-shock confluence then forms at t_n. In the hodograph diagram a gap opens at t_n and the maps of both t_j and n retreat from the sonic line locus as shown. The two separated segments of the map are joined by a polar which grows continuously as the gap opens. This polar is constructed for the Mach number $M_{1(n-l)}$ (l positive) and depends on how far r has climbed up t_j. With continued development r reaches the edge of the boundary layer as in figure 11*f*. In both planes the wave t_j has now shrunk into a point and the shock system is similar to the double Mach reflexion shown in figure 7*c*. At the next event (figure 11*g*), r has climbed up i and as a result n now extends into the main stream. This is the 'Mach reflexion' observed in a wind tunnel. With further development the Mach number downstream of i begins to approach unity, $M_{10} \to 1$, and eventually $M_{10} = 1$ as in figure 11*h*; r is then a sonic degeneracy. The last stages of the sequence are shown in figures 11*i* and 11*j* where $M_{10} < 1$ and i finally becomes normal to the flow at B.

Concurrently with the above events the lambda foot is growing under the influence of the steadily increasing downstream pressure. The confluence γ_2 passes up through the boundary layer until it reaches the edge as in figure 11*g*. With subsequent development the lambda foot extends into the main stream.

† Dropping the superscript.

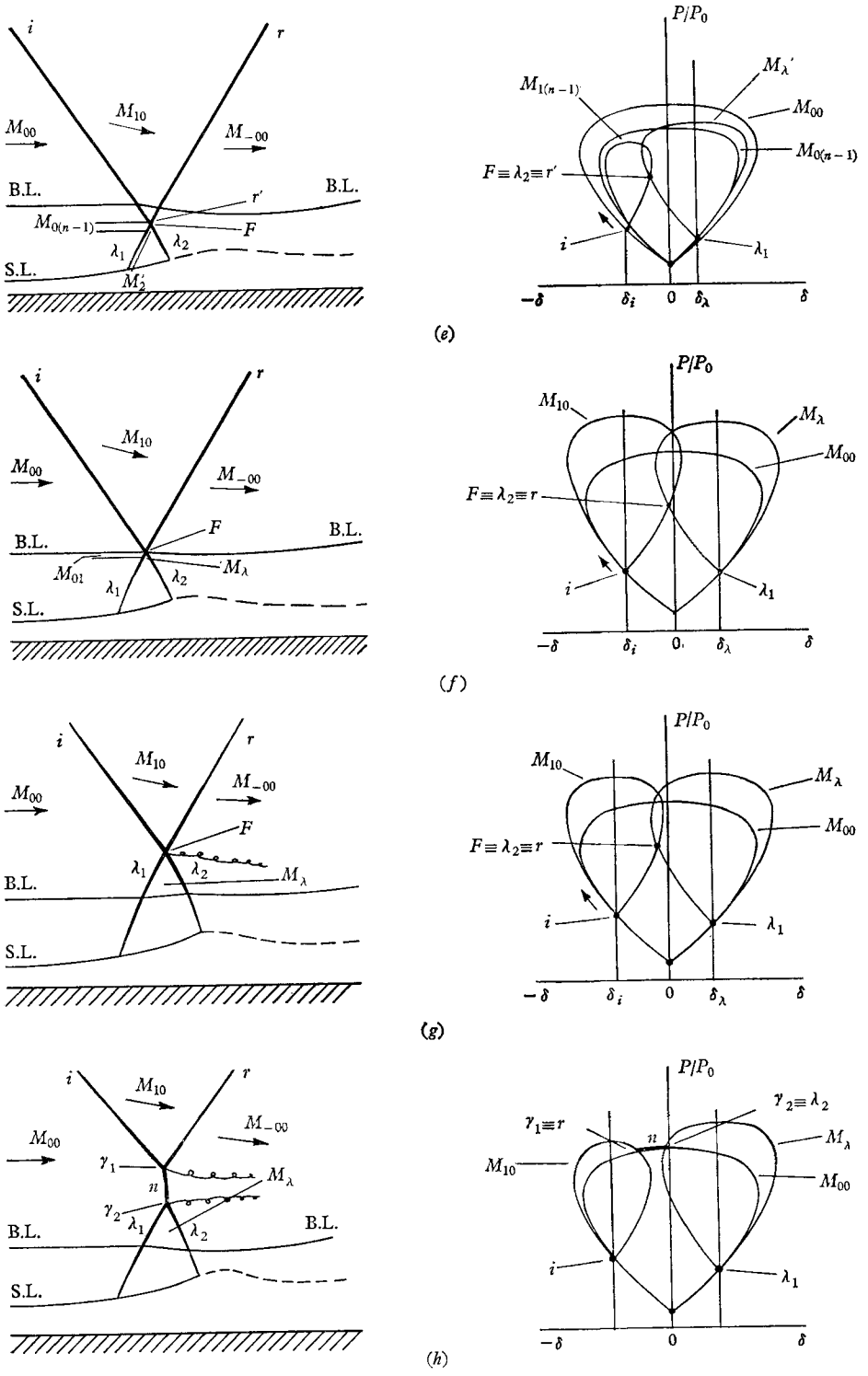

FIGURE 12. Development of irregular reflexion—alternative type.

The Mach reflexion may thus be observed with or without a lambda foot in the main stream. Liepmann *et al.* (1952) have observed it with a lambda foot (figure 13 of their paper), while Fage & Sargent (1947) appear to have observed both types (figure 5 of their paper). The hodograph diagram shows also that an alternative shock configuration is possible. This occurs if the polars $M_{1(n-1)}$ and M_λ intersect each other as shown in figure 12*e*; compare with figure 11*e* where they do not intersect. The wave system is then essentially a four-wave confluence type. Increasing the strength of i may force F into the main stream (figure 12*g*) and further development may change it into a Mach reflexion system (figure 12*h*). The rest of the sequence is similar to that shown in figure 11. A number of these events have been observed experimentally by Bardsley & Mair (1951) and in those experiments the refraction of the wave λ_2 is apparently producing a strong expansion. Other experimentalists who have observed the four-wave confluence are Liepmann *et al.* (1952), Gadd *et al.* (1954) and Bogdonoff & Kepler (1955).

In a broad sense it can now be said that there are actually two types of irregular reflexion in a real gas. On the one hand there is the sequence shown in figure 11 in which the Mach stem n is gradually extended into the main stream and is followed later by the extension of the lambda foot into the main stream. This sequence perhaps comes closest to the inviscid theory and will be called here 'Mach reflexion'. On the other hand, there is a sequence of the type shown in figure 12 in which the lambda foot is first extended into the main stream and the Mach stem develops from this system at a later stage. Both types of irregular reflexion can be said to commence once the shock r forms and starts to sweep upstream. This appears to happen at the condition where the downstream compression waves are deflecting the flow through the Prandtl–Meyer angle. The initial conditions for this critical state are shown in figure 13. The curve is based on the Prandtl–Meyer angle for the Mach number M_{10}. The curve obtained from the inviscid theory is shown for comparison. The definition of regular and irregular reflexion can now be restated as follows. The reflexion will be regular if the Mach stem and the lambda foot are confined to the boundary layer but it will be irregular if either extends into the main stream.

The sequences shown in figures 11 and 12 involve the tacit assumption that if there is separation of the boundary layer near the lambda foot then its influence is not sufficient to alter the described order of events. In practice this may not always be correct, as shown by experiments due to Bardsley & Mair (1951). Some of their experimental points have been plotted in figure 13 and it will be noted that the four-wave confluence appears in the main stream long before the Mach reflexion limit is attained. Inspection of the photographs published with their paper indicates that this is associated with the separation of the boundary layer. In this case the boundary layer was turbulent. The separation alters the sequences depicted in figures 11 and 12 by forcing the lambda foot into the main stream at an earlier stage in the development. The sequence would now read figures 11*a*, *b*, *e*, 12*e–h*, 11*h–j*. For laminar boundary layers Curle (1962) has discussed a variety of theoretical and experimental treatments of the problem of finding the pressure distribution that leads to

separation. The pressure coefficient at separation is given by expressions of the form:

$$c_P = 0{\cdot}93[(M_{00}^2 - 1)\,\mathrm{Re}]^{-\frac{1}{4}}. \tag{2}$$

It therefore appears that there are at least two ways for a regular system to become irregular. First, a shock may form downstream of the system and then sweep upstream as illustrated by the sequences of figure 11 or figures 11*a–e*, 12*e–h*, 11*h–j*. This is similar to the flow becoming 'unstarted' or disestablished as in supersonic wind tunnels and the criterion for its onset is shown in figure 13.

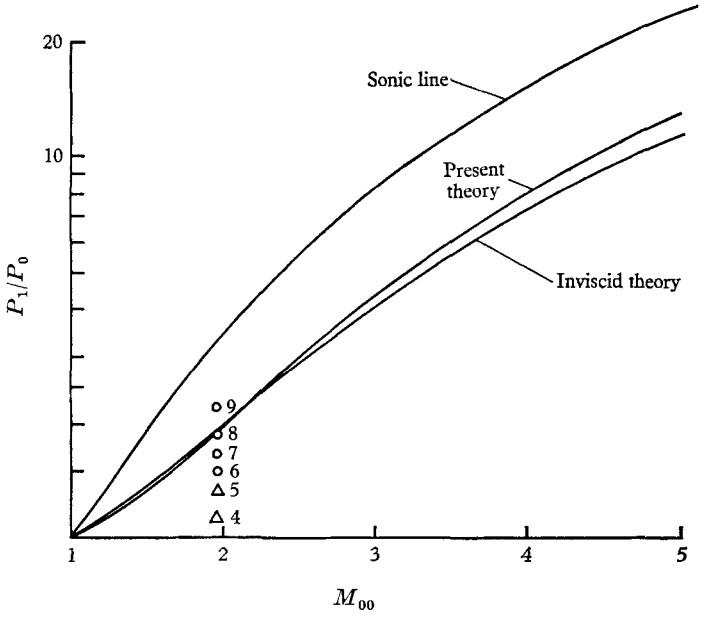

FIGURE 13. Conditions for the onset of Mach reflexion $\gamma = \frac{7}{5}$. Experiments (Bardsley & Mair 1951): △, four-wave confluence not visible; ○, four-wave confluence visible. Numbers refers to schlieren photographs in Bardsley & Mair's paper.

Secondly, the boundary layer may separate and force the lambda foot into the main stream: this is illustrated by the sequence, figure 11*a*, *b*, *e*, 12*e–h*, 11*h–j*. If the boundary layer is laminar at separation then the criterion for the onset of the phenomenon is equation (2); the criterion for turbulent separation is in a less satisfactory state. It would be interesting to repeat Bardsley & Mair's experiments at some other values of (M_{00}, Re) where separation is not so influential, the objective being to obtain the sequences shown in figures 11 and 12. In any event their experiments do confirm that the theoretical curve (figure 13) correctly predicts the appearance of the Mach stem *n* in the main stream. Thus figure 8 of their paper is a photograph of the flow precisely at the conditions corresponding to the theoretical curve (the point is plotted in figure 13 here). The existence of an incipient Mach stem is proved by the twin vortex sheets clearly visible in their photograph.

5. Upstream influence and viscous effects

From the picture of the flow presented so far it may be concluded that there will be no essential change in the wave system if the upstream boundary-layer profile is altered in any way that preserves the monotonic decrease in Mach number from the free stream to the wall. If, for example, the profile is gradually changed from laminar to turbulent then the effect is only to distort the wave system and not to alter its basic character. Significant differences do begin to appear, however, once the effects of upstream influence are taken into account. In experiments with laminar boundary layers an increase in wall pressure has been detected far upstream of the primary region of interaction. The subsonic part of the boundary layer gradually thickens as it approaches the lambda foot and this is often accompanied by separation upstream of the interaction zone. Compression waves are therefore generated along the upstream sonic line and are propagated into the main stream, where they interact with the incident shock i, causing it to strengthen (figure 9). The waves i, λ_1 will be then less clearly defined. The methods described here can in principle be used to deduce the structure of the wave system if the pressure distribution along the sonic line is given. The distribution is not known *a priori* and must be obtained from the theory of the subsonic part of the layer, and this is considered to be outside the scope of the present paper. The upstream influence is usually much smaller when the boundary layer is turbulent and may only extend a few displacement heights beyond the primary refraction zone. Evidently the reason for the difference is that the more vigorous mixing in the turbulent boundary layer enables a larger pressure gradient to be supported near the lambda foot.

Further sources of mixing are the Mach stem $t_j n$ and the lambda foot λ_1, λ_2, all of which emit continuous bands of vortex sheets. When the Mach number and the Reynolds number are large, the boundary layer may be very thin and the shocks inside it will be sharply curved. This means that the vortex sheets will be intense and they will cause vigorous mixing in the downstream part of the boundary layer. This suggests that, when there is a laminar profile upstream, the transition to turbulence will be strongly promoted by the action of the waves $t_j n \lambda_2$.

The general shape of the streamlines in the subsonic part of the boundary layer is also of interest. Referring again to figure 8 the sonic line passes underneath the lambda foot and then jumps to the rear of the Mach stem at t_n. The thickness of the subsonic layer is therefore increased discontinuously as it passes under the interaction zone. Furthermore, the sonic line is forced away from the wall in the upstream flow but towards the wall in the downstream flow. The effect is to induce a hump in the subsonic streamlines which presumably encourages the formation of the separation bubble. A few streamlines have been sketched to illustrate this feature.

6. Concluding remarks about some experiments

Of the various conclusions obtained from the theory it may be practical to test the following items by experiment.

(i) Is there a Mach stem $t_j n$ present during regular reflexion and if so is it bifurcated at its foot?

(ii) Are there two types of regular reflexion, namely one with reflected compression waves and the other with both reflected compression and expansion waves, and if so does figure 4 accurately predict the conditions for the appearance of both types?

(iii) Are there two types of irregular reflexion, namely one with a Mach stem containing a lambda foot and the other a four-wave confluence type?

(iv) In the absence of extensive boundary-layer separation does a regular reflexion change into an irregular reflexion by a process that involves the formation of a downstream shock wave which subsequently sweeps upstream, and if so does the curve in figure 13 accurately predict the onset of the phenomenon?

Appendix. Polar intersections for two parallel streams of gas of infinitesimal Mach number differences

From one-dimensional shock theory the equations of the polars are (δ streamline deflexion, P_1/P_0 shock pressure ratio)

$$\tan\delta_{00,01} = \frac{\alpha-1}{1+\gamma M_{00,01}^2-\alpha}\left[\frac{\frac{2\gamma}{\gamma+1}M_{00,01}^2-\frac{\gamma-1}{\gamma+1}-\alpha}{\frac{\gamma-1}{\gamma+1}+\alpha}\right]^{\frac{1}{2}}, \tag{A 1}$$

where $\alpha = P_{10,11}/P_{00,01}$.

At the polar intersections the following relations are valid:

$$\delta_{00} = \delta_{01}; \quad P_{10}/P_{00} = P_{11}/P_{01} = x. \tag{A 2}$$

Put $$b = 1+\gamma M^2; \quad c = \frac{\gamma-1}{\gamma+1}; \quad d = \frac{2\gamma}{\gamma+1}M^2-\frac{\gamma-1}{\gamma+1}.$$

Then from (A 1) and (A 2),

$$\frac{d_{00}-x}{(b_{00}-x)^2} = \frac{d_{01}-x}{(b_{01}-x)^2};$$

therefore

$$x^2[2(b_{01}-b_{00})+d_{00}-d_{01}]-x[b_{01}^2-b_{00}^2+2(b_{01}d_{00}-b_{00}d_{01})]+b_{01}^2d_{00}-b_{00}^2d_{01} = 0,$$

or, simplifying,

$$x^2-\tfrac{1}{2}(\gamma+1)(M_{00}^2+M_{01}^2)x-1+\gamma M_{00}^2M_{01}^2-\tfrac{1}{2}(\gamma-1)(M_{00}^2+M_{01}^2) = 0.$$

Therefore

$$x = \tfrac{1}{4}(\gamma+1)(M_{00}^2+M_{01}^2)\pm\tfrac{1}{2}\{(\tfrac{1}{2}[\gamma+1])^2(M_{00}^2+M_{01}^2)^2+4-4\gamma M_{00}^2M_{01}^2 + 2(\gamma-1)(M_{00}^2+M_{01}^2)\}^{\frac{1}{2}}.$$

Now let $M_{01} \to M_{00}$; then, after simplifying,

$$x \to \tfrac{1}{2}(\gamma+1)M_0^2 \pm (\tfrac{1}{2}(\gamma-1)M_0^2+1).$$

Therefore in the limit

$$x = 1+\gamma M_0^2, \text{ which is of no physical interest,}$$

or
$$x = M_0^2 - 1,$$

i.e.
$$\frac{P_{10,11}}{P_{00,01}} = M_0^2 - 1, \tag{A 3}$$

and in particular when $P_{10,11}/P_{00,01} = 1$ we have $M_0 = \sqrt{2}$. Hence at $M_0 = \sqrt{2}$ all polar intersections coincide with the polar double point.

REFERENCES

Ackeret, J., Feldmann, F. & Rott, N. 1946 *Mitt. Inst. Aerodyn. Zürich*, no. 10 (Zürich), or *Tech. Note Nat. Adv. Comm. Aero., Wash.* no. 1113.

Bardsley, O. & Mair, W. A. 1951 *Phil. Mag.* **42**, 39.

Barry, F. W., Shapiro, A. H. & Neumann, E. P. 1951 *J. Aero. Sci.* **18**, 229.

Bogdonoff, S. M. & Kepler, C. E. 1955 *J. Aero Sci.* **22**, 414.

Chapman, D. R., Kuehn, D. M. & Larson, H. K. 1958 *Rept. Nat. Adv. Comm. Aero., Wash.* no. 1356.

Curle, N. 1962 *The Laminar Boundary Layer Equations*. London: Oxford University Press.

Fage, A. & Sargent, R. F. 1947 *Proc. Roy. Soc.* A **190**, 1.

Gadd, G. E., Holder, D. W. & Regan, J. D. 1954 *Proc. Roy. Soc.* A **226**, 227.

Guderley, K. G. 1947 *Tech. Rept. Headquarters Air Materiel Command, Wright Field, Dayton, Ohio*, no. F–TR–2168–ND.

Guderley, K. G. 1962 *The Theory of Transonic Flow*. Oxford: Pergamon Press.

Hakkinen, R. J., Greber, I. & Trilling, L. 1959 *Memo. Nat. Aero. and Space Admin., Wash.* no. 2–18–59W.

Henderson, L. F. 1966 *J. Fluid Mech.* **26**, 607.

Henderson, L. F. 1967 *J. Fluid Mech.* (in the press).

Holder, D. W. & Gadd, G. E. 1955 *Boundary Layer Effects in Aerodynamics*. London: Her Majesty's Stationery Office.

Jahn, R. G. 1956 *J. Fluid Mech.* **1**, 457.

Kawamura, R. & Saito, H. 1956 *J. Phys. Soc. Japan*, **11**, 584.

Lees, L. & Reeves, B. L. 1964 *A.I.A.A. J.* **2**, 1907.

Liepmann, H. W. 1946 *J. Aero. Sci.* **13**, 623.

Liepmann, H. W., Roshko, A. & Dhawan, S. 1952 *Rept. Nat. Adv. Comm. Aero., Wash.* no. 1100.